

CRITICAL PHENOMENA AT THE
SURFACE OF SYSTEMS UNDERGOING A
BULK FIRST ORDER TRANSITION: ARE
THEY UNDERSTOOD?

*** Dedicated to David Landau ***
on occasion of his 60th birthday

K. Binder¹, F. F. Haas¹, and F. Schmid²

¹Institut für Physik, Johannes Gutenberg Universität Mainz,
Staudinger Weg 7, D-55099 Mainz, Germany

²Theoretische Physik, Universität Bielefeld, D-33602 Bielefeld, Germany

March 19, 2001

ABSTRACT Systems that exhibit a first-order phase transition in the bulk, such as binary alloys where the order parameter vanishes discontinuously at some critical value of a control parameter, may show a continuous vanishing of the local order parameter at the surface. This “surface-induced disordering” is described theoretically as a variant of critical wetting, where an interface between the locally disordered surface and the ordered bulk gradually moves towards the bulk. We test this description by Monte Carlo simulations for a body centered cubic model alloy, with interactions between nearest and next nearest neighbors, for which the phase diagram in the bulk has been calculated very accurately. A critical vanishing of the order parameter components is found both for the (110) and the (100) surface. In contrast to the theory, the simulations indicate different critical exponents ν from the order parameter of the B2 phase and the order parameter of the DO₃ phase. Observations from simulations for the face centered cubic lattice and from experiments are also briefly discussed.

1 Introduction

Critical behavior at surfaces of systems that undergo a second-order phase transition has found extensive attention during the last thirty years and is now rather well understood [1, 2, 3, 4]. Although first-order phase transitions are much more common in nature, their surface effects have received much less attention so far: from a theorist’s perspective, the lack of a diverging correlation length in the bulk makes them much less interesting [5], and thus, it came later - and as much of a surprise! - when Lipowsky [6] discovered that a critical vanishing was possible for the order parameter at the surface of a system that exhibited a discontinuous transition in the bulk.

It turns out that solid binary alloys undergoing order-disorder transitions in the bulk (such as Cu-Au and Fe-Al alloys [5, 7]) should be suitable systems to observe this “surface induced disordering” (SID) [6], and some corresponding observations were in fact reported [8, 9, 10, 11] (even before there was a theoretical explanation [8]). Unfortunately, the quantitative interpretation of such experiments is often difficult due to various complications (e.g., crystallographic surface roughness, surface steps, chemisorbed impurities, etc.), and due to the fact that the microscopic interactions between the atoms are neither known accurately in the bulk nor near the surface. Thus, it is very desirable to study this problem with computer simulations: In a computer experiment, we can provide an absolutely perfect, rigid surface (Fig. 1), all the interactions of a model can be chosen at will and are hence precisely known [12].

In fact, surfaces of binary alloys were studied in terms of an Ising model by David Landau and one of the present authors already 25 years ago [13], but there the model was restricted to a nearest neighbor interaction. For simple cubic (sc) and body centered cubic (bcc) lattices, only second

order transitions are then possible in the bulk [14, 15]. However, first order transitions do occur for nearest neighbor face-centered cubic (fcc) lattices, which provide a crude model for Cu-Au alloys [14, 15]. It turns out that a (100) surface of this model is an example for surface-induced ordering (SIO) [6], since the surface is less “frustrated” than the bulk [16, 17], and hence two-dimensional order in the surface plane sets in at a temperature that is higher than the ordering temperature of the bulk. Only when the surface plane is a (close-packed) (111)-plane, does SID occur [17].

Here we shall focus exclusively on the case of the bcc lattice, where one finds both the B2 structure and the DO_3 structure, if interactions (which disfavor occupancy by atoms of the same type) both between nearest and between next nearest neighbors are allowed for [18, 19]. Surface-induced disordering in this model has now been studied since 10 years already [20, 21], but as we shall see below, important questions still remain open.

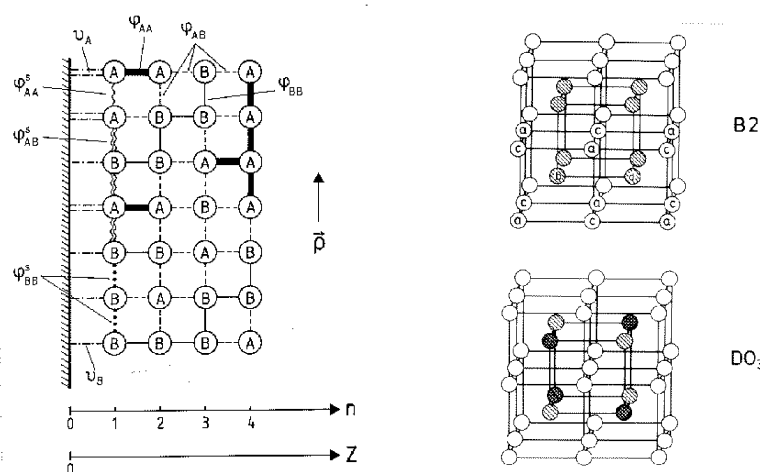


Figure 1:

Left: Schematic picture of the surface of a binary (AB) alloy at $z = 0$ (the shading indicates that this may represent an inert hard wall). Different nearest-neighbor interactions between different atoms (circles) or between atoms and the wall are indicated by different types of lines. For a discrete description, lattice planes parallel to the surface are labelled by positive integers n , while in the continuum description c coordinates parallel (ρ) and perpendicular (z) to the surface are used, as indicated. Right: Body centered cubic lattice showing the B2 structure (upper part) and the DO_3 structure (lower part). The assignment of four sublattices a, b, c, d is indicated. These structures (B2, DO_3) as well as the disordered A2 structure (random occupation of lattice sites by the two kinds of atoms in the binary alloy) occur in the Fe-Al-system.

In Sec. 2, we shall briefly review the theoretical background about SID, while Sec. 3 explains the model and comments about our simulation methods. Sec. 4 summarizes our main results, while Sec. 5 gives our conclusions.

2 Theoretical background

On a qualitative level, surface-induced disordering can already be understood within a simple Landau theory [6]. If one has only a single component order parameter (m), the free energy functional $\mathcal{F}(m)$ can be written as

$$\mathcal{F}\{m\} = \int_0^\infty dz \left\{ f_b(m) + \frac{g}{2} \left(\frac{dm}{dz} \right)^2 \right\} + f_s(m(z=0)), \quad (1)$$

where $f_b(m)$ is the free energy density of the bulk, $g > 0$ is a constant (the term $g(dm/dz)^2/2$ describes the free energy cost of order parameter inhomogeneities), and f_s is a (bare) surface free energy (assuming short range interactions with the surface). Taking, e. g.,

$$f_b(m) = \frac{r}{2}m^2 - \frac{u}{4}m^4 + \frac{v}{6}m^6, \quad (2)$$

with coefficients $r, u, v > 0$, a first order transition occurs in the bulk at [5] $r_c = 3u^2/(16v)$ where the order parameter m_b jumps discontinuously from zero (for $r > r_c$) to $m_b = \pm(3u/4v)^{1/2}$ for $r < r_c$.

In the presence of the free surface, Eq. (1) is minimized by the bulk equation

$$g d^2m/dz^2 = \partial f_b/\partial m \quad (3)$$

subject to the boundary condition at $z = 0$

$$g dm/dz = -\partial f_s(m)/\partial m \quad \text{with} \quad \left| g \frac{dm}{dz} \right| = \sqrt{2gf_b(m)}. \quad (4)$$

Assuming that the surface does not discriminate between the two signs of the order parameter, the simplest choice for $f_s(m)$ is $f_s(m) = \frac{1}{2}cm^2$ [1, 2, 3]. Then the solution of Eq. (4), which yields the order parameter $m_1 \equiv m(z=0)$ at the surface, is found from an analogue of the Cahn construction [22] for wetting phenomena [23], see Fig. 2. One can see that for large enough c the solution for m_1 moves continuously to zero as $r \rightarrow r_c^-$ (when the middle minimum of $f_b(m)$ for $m = 0$ becomes equally deep as the minima for $\pm m_b$). Working out the algebra, Eqs. (2)-(4), one finds (for $c > \sqrt{gr_c}$)

$$m_1 \propto (r_c - r)^{\beta_1}, \quad \beta_1 = 1/2. \quad (5)$$

Physically, this behavior can be interpreted in terms of a layer of the disordered phase intruding from the surface into the bulk near r_c (Fig. 3). The interface between this disordered layer and the ordered phase has an intrinsic width $w_0 = 2\xi_b$ and its center is at an average distance L from the surface, and as $r \rightarrow r_c$ this distance diverges (Fig. 3).

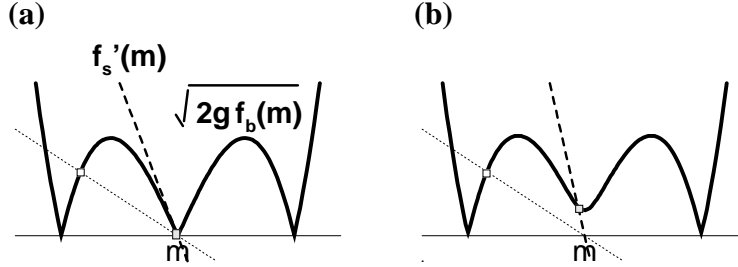


Figure 2:

Cahn construction (schematic) for surface-induced disorder in a system with a one component order parameter m at bulk coexistence (a) and off coexistence and (b). Dashed line shows surface term $f'_s(m) = \partial f_s(m)/\partial m = cm$ for critical wetting; dotted line for partial wetting. From Haas et al. [20].

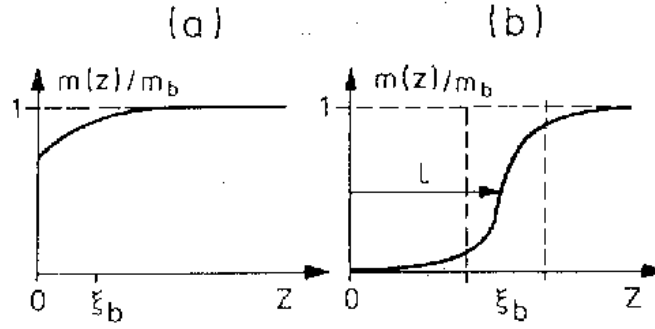


Figure 3:

Order parameter profiles $m(z)/m_b$ associated with SID. If case (a) persists up to r_c , the surface stays ordered at r_c , only some reduction of $m(z)$ over a range of the bulk correlation range ξ_b occurs. Case (b) shows SID: a layer of thickness L has disordered already at $r < r_c$, and as $r \rightarrow r_c$, the interface (at mean position $z = L$) advances into the bulk, according to $L \propto |\ln(r_c - r)|$ for short range surface forces. The surface order parameter $m_1 = m(z = 0)$ then vanishes continuously according to Eq. (5). From Dosch et al. [11].

So far our discussion has been strictly on the mean field level. Since the bulk of the system is not critical, one can expect fluctuations to be negligible, apart from fluctuations of the local position $\ell(\vec{\rho})$ of the interface between the disordered surface layer and the ordered phase in the bulk ($\vec{\rho}$ is a coordinate in the directions parallel to the surface). As the interface moves into the bulk, capillary-wave-type excursions of larger and larger wavelength become possible. These introduce long-range correlations parallel to the surface, up to the length scale $\xi_{||}$ which diverges at r_c .

These considerations motivate the use of the effective interface Hamiltonian,

$$\mathcal{H}_{eff}\{\ell\}/k_B T = \int d\vec{\rho} \left\{ \frac{1}{8\pi\omega} (\nabla\ell)^2 + V_0(\ell) \right\}, \quad (6)$$

where the capillarity parameter ω is a dimensionless constant related to ξ_b and the interfacial tension σ , $\omega = k_B T / [4\pi\sigma\xi_b^2]$, and the potential $V_0(\ell)$ describes effective interactions between the interface and the surface. SID is identified as a depinning of the interface from the surface. The effective potential $V_0(\ell)$ can be written as [6]

$$V_0(\ell) \propto \exp(-2\ell/\xi_b) + t\ell, \quad t \propto r_c - r \quad (7)$$

A renormalization group treatment [24] of Eq. (6) then gives [6]

$$\bar{\ell} \equiv \langle \ell \rangle \propto \xi_b t^{-\beta_s}, \quad \xi_{||} \propto \xi_b t^{-\nu_{||}}, \quad \xi_{\perp} \propto \xi_b t^{-\nu_{\perp}} \quad (8)$$

with ξ_{\perp} describing the interfacial width (or roughness, respectively) and the exponents β_1 , β_s , $\nu_{||}$ and ν_{\perp} (for $0 \leq \omega < 1/2$) [6]

$$\beta_1 = (1 + \omega)/2, \quad \beta_s = 0(\log), \quad \nu_{||} = 1/2, \quad \nu_{\perp} = 0(\log). \quad (9)$$

More precisely, one finds $\bar{\ell}/\xi_b = (1/2 + \omega) \ln(1/t)$, $\xi_{\perp}/\xi_b = \sqrt{\omega} [\ln(1/t)]^{1/2}$ [6].

A caveat important for the present case, however, is that the theory summarized above should hold for the case of a single-component order parameter. As will be discussed below, the DO₃ ordering on the bcc lattice is described by three order parameter components [18]. The extension of the mean-field theory of SID to order parameters with several components shows that deviations from $\beta_1 = 1/2$ (Eq. (5)) may occur already at the mean field level [25, 26]. However, a more detailed analysis reveals that such deviations are only likely at surfaces which break the symmetry of the order parameter [21]. A renormalization group analysis [21] suggests that Eqs. (8), (9) remain valid asymptotically also in the case of several order parameters at symmetry preserving surfaces (such as the (110) surface of the bcc-lattice, see below), although the critical region may become much narrower. Furthermore, the critical exponent $\nu_{||}$ should be $\nu_{||} = 1/2$ under all circumstances.

3 Model and simulation methods

We now focus on binary alloys (AB) on the body centered cubic (bcc) lattice with the ordered structures already shown in Fig. 1. Dividing the bcc lattice into four sublattices a, b, c, d as indicated, one denotes by c_α the average concentration of component A on sublattice α . Then order parameter components Ψ_1, Ψ_2, Ψ_3 are defined as [18]

$$\begin{aligned}\Psi_1 &= (c_a - c_b + c_c - c_d) \\ \Psi_2 &= (c_a + c_b - c_c - c_d) . \\ \Psi_3 &= (c_a - c_b - c_c + c_d)\end{aligned}\quad (10)$$

While $\Psi_1 = \Psi_2 = \Psi_3 = 0$ in the disordered (A2) phase, $\Psi_1 \neq 0$ in the phase with B2 order, and all three components nonzero with $\Psi_2 = \pm\Psi_3$ in the DO₃ phase. Symmetry agreements lead to the Landau expansion [20, 21]

$$\begin{aligned}f_b &= f_0 + A_1\Psi_1^2 + A_2(\Psi_2^2 + \Psi_3^2) + B\Psi_1\Psi_2\Psi_3 + C_1\Psi_1^4 + C_2(\Psi_2^4 + \Psi_3^4) \\ &\quad + C_3\Psi_2^2\Psi_3^2 + C_4\Psi_1^2(\Psi_2^2 + \Psi_3^2)\end{aligned}\quad (11)$$

Note that a cubic term $B\Psi_1\Psi_2\Psi_3$ exists which couples all three components together: when Ψ_2, Ψ_3 become nonzero, the term $\Psi_2\Psi_3B$ acts like an effective ordering field on the order parameter Ψ_1 of B2-order.

Considering free surfaces, it is important to realize that the surface free energy depends on the orientation of the surface. First, one component will always be enriched at the surface: there are no symmetry arguments to prevent that. Second, only the (110) surface has the same symmetry with respect to sublattice exchanges as the bulk, and then f_s has an expansion of the same form as f_b . For a (100) surface, however, the symmetry with respect to the exchange of sublattices $(a, c) \leftrightarrow (b, d)$ is broken. The surface enrichment of one component then induces an effective ordering surface field h_1 , which couples to the order parameter Ψ_1 [27]. Other ordering fields coupling to Ψ_2 and Ψ_3 are still forbidden by symmetry, while they would be allowed (and thus in general nonzero) for the case of (111) surfaces [21].

These orderings and phase transitions between them can be simply obtained from an Ising model with "antiferromagnetic" interactions V between nearest and V_{nnn} between next nearest neighbors [18, 19, 20, 21],

$$\mathcal{H} = V \sum_{\langle i, j \rangle nn} S_i S_j + V_{nnn} \sum_{\langle i, j \rangle nnn} S_i S_j - H \sum_i S_i, \quad S_i = \pm 1, \quad (12)$$

where $V_{nnn}/V = 0.457$ was chosen such that the highest temperature which can still support a B2 phase is about twice as high as the highest temperature of the DO₃ phase, as experimentally observed in the Fe-Al system. Note that the concentration of the alloy is simply related to the average magnetization per spin, $c = (1 + \langle S_i \rangle)/2$, and the field H is related to the

chemical potential difference $\mu_A - \mu_B$ of the alloy [14, 15, 18]. As discussed extensively in the literature [14, 15, 18], it is much more convenient to carry out simulations in this “semi-grand canonical ensemble” of the alloy, rather than in the canonical ensemble with fixed c as an independent variable. Since all ensembles are equivalent in the thermodynamic limit, one can easily translate the results from one ensemble to the other.

Thus, we show here results in the “semi-grandcanonical ensemble” only, where H is an independent variable (like the temperature T). Fig. 4 shows the phase diagram in the bulk [21]. For this study, a multispin coding single spin flip Metropolis program was implemented on an INTEL PARAGON parallel processor at the HLRZ Jülich, using lattices up to $80 \times 80 \times 80$ and domain decomposition as a standard method of geometric parallelization [28]. Data analysis was done with standard histogram reweighting [12, 29] and finite size scaling [12, 30, 31] techniques.

Thus, second-order transitions could be located precisely by the crossings of the fourth order cumulant of the respective order parameter, and weak first-order transitions (as they occur near the tricritical point) were found from the “equal weight rule”. Strong first-order transitions such as the DO_3 -A2 transition at low temperatures were located by obtaining the free energy of the two phases as a function of H via thermodynamic integration [12, 32]. It turned out that the first-order DO_3 -B2 transition was rather weak even at the critical end point, due to the proximity of the tricritical point (Fig. 4). A study of SID at such weak 1st order transitions would require system sizes so huge that it is still not yet feasible today.

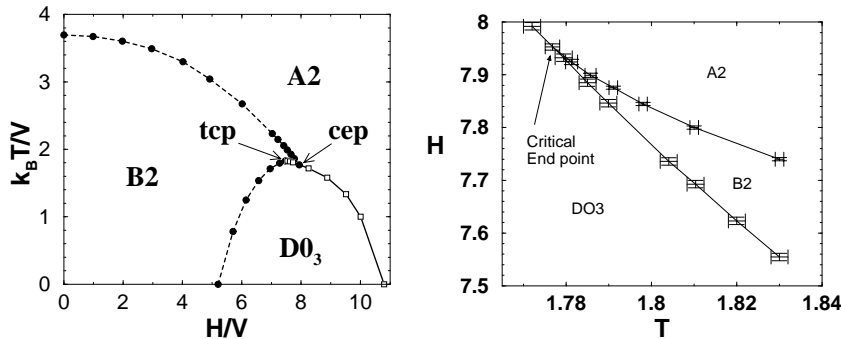


Figure 4:

Left: Global phase diagram of our model {Eq. (12)} in the $T - H$ plane (left part), indicating the three phases. Solid lines mark first-order transitions; dashed lines second-order transitions. Arrows indicate the positions of a critical end point (cep) and a tricritical point (tcp). Right: Magnification of the part of the phase diagram near the cep, including error bars to show the accuracy with which such phase boundaries can be determined.

Therefore we focus on the DO₃-A2 transition at $k_B T/V = 1$, where the transition occurs at $H_0/V = 10.00771$ (1) [21, 28]. Note that more than 10^3 different states were used for the integration to reach this very good accuracy.

The surface simulations were then performed in a $L \times L \times D$ geometry, with periodic boundary conditions in the L direction and free boundary conditions in the D direction. We varied D from 100 to 200 (to check that finite size effects associated with D are negligible) and L from 20 to 100 (to carry out a finite size scaling analysis with L). Runs of a total length of up to 2×10^6 Monte Carlo sweeps were carried out.

4 Simulation results and analysis

We first focus on free (110) surfaces and discuss the “profiles” of the order parameter $\Psi_{23} = [(\Psi_2^2 + \Psi_3^2)/2]^{1/2}$, Fig. 5. Note that the strong field H implies that the very top layer of a free surface is completely filled with A atoms, i.e. all Ising spins $S_i = +1$ in that layer, and all order parameters Ψ_α vanish there. Thus, unlike sketched in Fig. 1, we label our layers $n = 1, 2, \dots$ starting out from the second layer, the top layer is $n = 0$. One sees from Fig. 5 that the layers near the surface become more and more disordered as $H \rightarrow H_0$, and an interface forms and moves towards the bulk.

We can fit the profile by the function

$$\Psi_{23}(n) = \Psi_{23}^{bulk} \{1 + \exp[-2(z - \langle \ell \rangle)/W]\}^{-1} \quad (13)$$

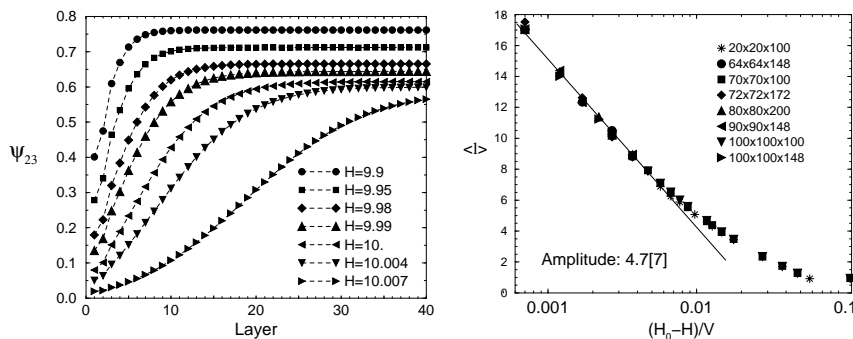


Figure 5:

Left: Profiles of Ψ_{23} near a (110) surface at temperature $k_B T/V = 1$ for different fields H (in units of V) as indicated. Right: Position of the interface $\langle \ell \rangle$ as estimated from a fit to Eq. (13) plotted vs. the reduced distance from the bulk transition field [21].

to extract both the interface position $\langle \ell \rangle$ (Fig. 5) and the width (Fig. 6). Near H_0 the data is indeed compatible with the predicted logarithmic divergence of $\langle \ell \rangle$ and W^2 , in the regime where $\langle \ell \rangle$ exceeds W (Fig. 6). However, the small range of $(H_0 - H)/V$ where the logarithm can be fitted to the data does not warrant a detailed discussion of the prefactors in that law [21].

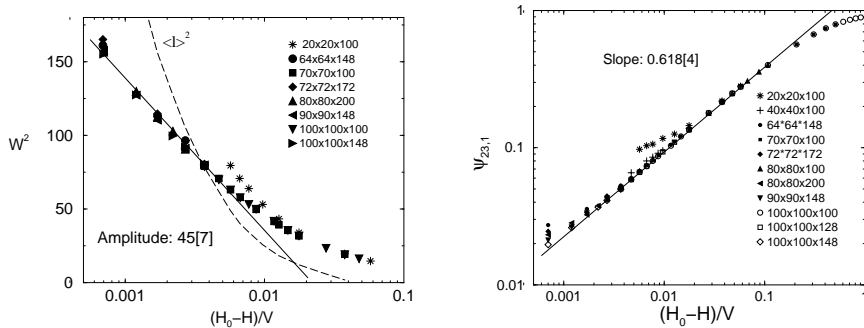


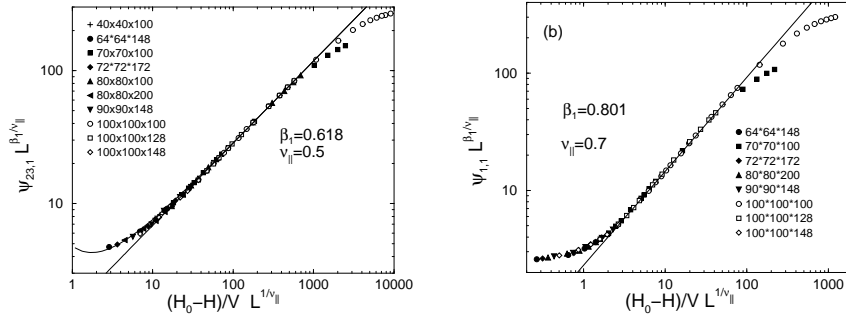
Figure 6:

Left: Squared interfacial width as estimated from Eq. (13) plotted vs. $(H - H_0)/V$. Long dashed line shows squared interface position $\langle \ell \rangle^2$ for comparison. Right: Order parameter $\Psi_{23,1}$ adjacent to the surface planes $(H - H_0)/V$ for different system sizes $L \times L \times D$ as indicated. Solid line is the power law Eq. (5) with $\beta_1 = 0.618$. From Haas et al. [21].

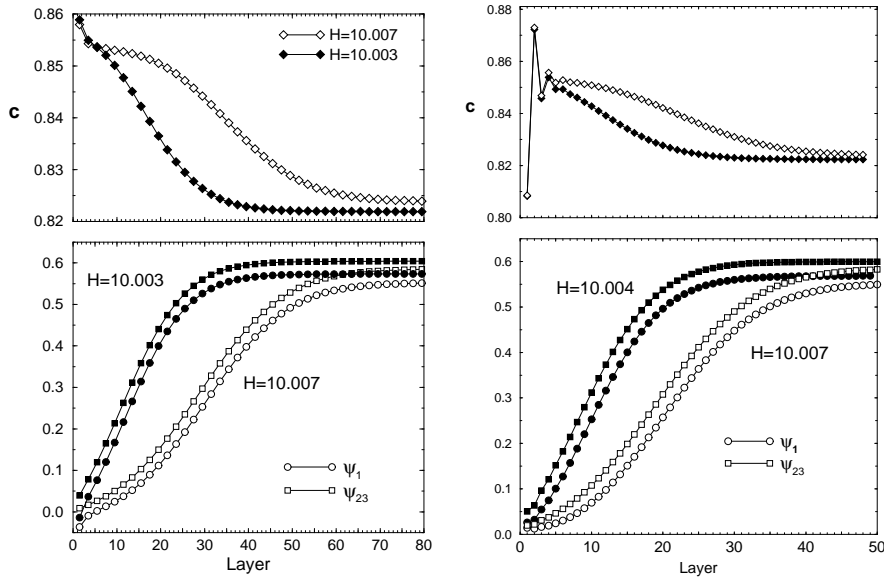
Finally, the order parameter $\Psi_{23,1}$ in the layer adjacent to the surface (Fig. 6) is compatible with Eq. (5) but the exponent β_1 is $\beta_1 \approx 0.618$, implying $\omega = 0.236$ {Eq. (9)} [21]. This value happens to be similar to β_1 for the (111) surface of the fcc antiferromagnetic Ising model [17].

From Fig. 6 (right part) one can clearly recognize that the data for small L and small $(H_0 - H)/V$ deviate from the power law. These “finite-size tails” can be nicely accounted for by a finite size scaling analysis (Fig. 7), using the theoretical exponent $\nu_{||} = 1/2$ {Eq. (9)}. However, an analogous analysis for the order parameter Ψ_1 yields different exponents, $\beta_1 = 0.8$, and $\nu_{||} = 0.7$ (Fig. 7). While several surface exponents β_1 may occur in systems with several order parameter components under certain conditions [21, 25, 26], $\nu_{||}$ should remain invariably $\nu_{||} = 1/2$. We have no explanation for this unexpected discrepancy between simulation and theory.

Finally, we comment on (100) surfaces where an ordering field coupling to Ψ_1 is present. This is demonstrated in Fig. 8, where the profiles of the order parameters and the composition c are defined based on the sublattice occupancies on two subsequent layers of distance $a_0/2$, starting from the first layer adjacent to the surface plane (the latter is again disregarded, since it is entirely filled with A , $c = 1$). The profiles of Ψ_1 show the signature of

**Figure 7:**

Left: Finite-size scaling plot of the surface order parameter $\Psi_{23,1}$ vs. $(H_0 - H)/V$ for system sizes $L \times L \times D$ as indicated. Data were scaled with exponents $\nu_{||} = 1/2$ and $\beta_1 = 0.618$. Curve shows a theoretical scaling function derived in [21]. The asymptotic power law is shown by a straight line. Right: Finite size scaling plot of the order parameter Ψ_1 . Optimal data collapse occurs for $\beta_1 = 0.801$ and $\nu_{||} = 0.7$. From Haas et al. [28]

**Figure 8:**

Left: Profiles of the total concentration c of A (top) and the order parameters Ψ_1 , Ψ_{23} (bottom) for a (100) surface at $H/V = 10.003$ (filled symbols) and at $H/V = 10.007$ (open symbols). Right: Same as left part, but for a (110) surface.

an effective ordering surface field H_1 , induced by the surface segregation of A [27]. This field in fact reverses the sign of Ψ_1 in the top layers, which does not happen at (110) surfaces (Fig. 8, right part). However, the effect is rather weak and does not influence the system significantly deeper in the bulk. The profiles are very similar to those of the (110) surface, and their analysis yields very similar results, including an exponent $\beta_1 = 0.61$ for the power law (Eq. (5)) of the order parameter $\Psi_{23,1}$.

5 Conclusions

In the work described here, SID was simulated for the phase transition of ordered bcc alloys from the DO_3 structure (like Fe_3Al) to the disordered phase. This study is similar in spirit to related work by Schweika et al. [17] for the (111) surface of fcc alloys. In the latter case, however, a 50:50 composition with $\mu_A - \mu_B = 0$ was studied, and neither surface enrichment nor surface-induced ordering fields H_1 did occur, unlike in the present model (Fig. 8). In addition, we find here that the coupling between the (nonequivalent) order parameters Ψ_1 and Ψ_{23} seems to give rise to novel features, see Fig. 7 for an example. As emphasized above, the critical behavior of Ψ_1 at the SID transition is not at all understood.

Hence, already this simple model, highly idealized in comparison with real alloys, exhibits a complex behavior. In real alloys, we expect additional complications due to long range elastic interactions, giving rise to lattice distortions near the surface. Also the surface roughness of real surfaces (steps, islands, etc.) may play an important role; note that on a symmetry breaking surface, every step changes the sign of the field H_1 . The available experiments [8, 9, 10, 11] have concentrated on the case of Cu_3Au and can hence neither be compared to this work nor directly to the study by Schweika et al. [17] Clearly, both additional experiments (searching for SID in bcc alloys) and simulations (careful studies of SID for a model of Cu_3Au) would be very desirable.

Acknowledgements: One of us (K. B.) is particularly indebted to David P. Landau for a longstanding and fruitful collaboration on closely related subjects (Refs. [13, 16, 17, 20]) from which the work here has strongly profited. Useful discussions with him and with B. Dünweg, R. J. Evans, M. Müller, A. O. Parry and W. Schweika are acknowledged. F. F. H. received support by the Graduiertenförderung of the Land Rheinland-Pfalz and F. S. from the Deutsche Forschungsgemeinschaft through the Heisenberg program when this work was done. A generous grant of computing time from the HLRZ Jülich is also acknowledged.

6 REFERENCES

- [1] K. Binder and P. C. Hohenberg, Phys. Rev. **B6**, 3461 (1972); **B9**, 2194 (1974)
- [2] K. Binder, in: *Phase Transitions and Critical Phenomena, Vol 8*, Eds. C. Domb and J. L. Lebowitz (Academic Press, London, 1983), p. 1
- [3] H. W. Diehl, in: *Phase Transitions and Critical Phenomena, Vol 10*, Eds. C. Domb and J. L. Lebowitz (Academic Press, London, 1986) p. 75
- [4] H. W. Diehl, Int. J. Mod. Phys. **B11**, 3503 (1997)
- [5] K. Binder, Progr. Theor. Phys. **50**, 783 (1987)
- [6] R. Lipowsky, Phys. Rev. Lett. **49**, 1575 (1982); J. Appl. Phys. **55**, 2485 (1984); Ferroelectrics **73**, 69 (1987)
- [7] M. Hansen, *Constitution of Binary Alloys* (Mc Graw Hill, New York 1958)
- [8] V. S. Sundaram, B. Farrell, R. S. Alben, and W. D. Robertson, Phys. Rev. Lett. **31**, 1136 (1973); V. S. Sundaram, R. S. Alben, and W. D. Robertson, Surf. Sci. **46**, 653 (1974)
- [9] E. G. McRae and R. A. Malic, Surf. Sci. **148**, 551 (1984)
- [10] S. F. Alvarado, M. Campagna, A. Fattah, and W. Uelhoff, Z. Phys. **B66**, 103 (1987)
- [11] H. Dosch, L. Mailänder, A. Lied, S. Peisl, F. Grey, R. L. Johnson and S. Krummacher, Phys. Rev. Lett. **60**, 2382 (1988); H. Dosch, L. Mailänder, H. Reichert, J. Peisl and R. L. Johnson, Phys. Rev. **B43**, 13172 (1991)
- [12] D. P. Landau and K. Binder, *A Guide to Monte Carlo Simulations in Statistical Physics* (Cambridge University Press, Cambridge, 2000).
- [13] K. Binder and D. P. Landau, Surface Sci. **61**, 577 (1976)
- [14] K. Binder, in *Festkörperprobleme (Advances in Solid State Physics)*, Ed. P. Grosse (Vieweg, Braunschweig, 1986) p. 133
- [15] K. Binder, in *Statics and Dynamics of Alloy Phase Transformations*, Eds. P. E. A. Turchi and A. Gonis (Plenum Press, New York, 1994) p. 467.
- [16] W. Schweika, K. Binder, and D. P. Landau, Phys. Rev. Lett. **65**, 3321 (1990)

- [17] W. Schweika, D. P. Landau, and K. Binder, Phys. Rev. **B53** , 8937 (1996)
- [18] B. Dünweg and K. Binder, Phys. Rev. **B36**, 6935 (1987)
- [19] F. Schmid and K. Binder, J. Phys.: Condens. Matter **4**, 3569 (1992)
- [20] W. Helbing, B. Dünweg, K. Binder and D. P. Landau, Z. Physik **B80**, 401 (1990)
- [21] F. F. Haas, F. Schmid, and K. Binder, Phys. Rev. **B61**, 15077 (2000)
- [22] J. W. Cahn, J. Chem. Phys. **66**, 3667 (1977)
- [23] S. Dietrich, in: *Phase Transitions and Critical Phenomena, Vol 12*, Eds. C. Domb and J. L. Lebowitz (Academic Press, London, 1988), p. 1
- [24] E. Brézin, B. I. Halperin, and S. Leibler, Phys. Rev. Lett. **50**, 1387 (1983)
- [25] E. H. Hauge, Phys. Rev. **B33**, 3322 (1986)
- [26] D. M. Kroll and G. Gompper, Phys. Rev. **B36**, 7078 (1987)
- [27] F. Schmid, in: *Stability of Materials*, Eds. A. Gonis, P. E. A. Turchi and J. Kudrnovsky, (Plenum Press, New York, 1996) p. 173.
- [28] F. F. Haas, *Oberflächeninduzierte Unordnung in binären bcc Legierungen* (Dissertation, Johannes Gutenberg-Universität Mainz, 1998)
- [29] A. M. Ferrenberg and R. H. Swendsen, Phys. Rev. Lett. **61** , 2635 (1988); *ibid* **63**, 1195 (1989)
- [30] K. Binder, Z. Phys. **B43**, 119 (1981); Phys. Rev. Lett. **47**, 681 (1981)
- [31] K. Vollmayr, J. D. Reger, M. Scheucher, and K. Binder, Z. Phys. **B91**, 113 (1993)
- [32] K. Binder, Z. Phys. **B45**, 61 (1981)